JPL PUBLICATION 86-44 (MSAT-X REPORT NO. 141)

Multiple Trellis Coded Modulation (MTCM)

An MSAT-X Report

D. Divsalar
M.K. Simon

November 15, 1986

National Aeronautics and
Space Administration

Jet Propulsion Laboratory
California Institute of Technology
Pasadena, California

JPL PUBLICATION 86-44 (MSAT-X REPORT NO. 141)

Multiple Trellis Coded Modulation (MTCM)

An MSAT-X Report

D. Divsalar
M.K. Simon

November 15, 1986

National Aeronautics and
Space Administration

Jet Propulsion Laboratory
California Institute of Technology
Pasadena, California

The research described in this publication was carried out by the Jet Propulsion Laboratory, California Institute of Technology, under a contract with the National Aeronautics and Space Administration.

Abstract

Conventional trellis coding outputs one channel symbol per trellis branch. Here we introduce the notion of multiple trellis coding wherein more than one channel symbol per trellis branch is transmitted. It is shown that the combination of multiple trellis coding with M-ary modulation yields a performance gain with symmetric signal sets comparable to that previously achieved only with signal constellation asymmetry. The advantage of multiple trellis coding over the conventional trellis coded asymmetric modulation technique is that the potential for code catastrophe associated with the latter has been eliminated with no additional cost in complexity (as measured by the number of states in the trellis diagram).

CONTENTS

Figures

Tables

1. Introduction

Trellis coded modulation (TCM) refers to the technique wherein a rate n/(n+1) trellis code is combined (through a suitable mapping function [1]) with an $M = 2^{n+1}$-point signal constellation to produce a coded modulation which has no bandwidth expansion relative to an uncoded 2^n-point modulation of the same type yet gives significant performance improvement.

Traditionally, TCM systems have employed symmetric signal constellations, i.e., those with uniformly spaced signal points. Examples of such for multiple phase-shift-keying (MPSK) and quadrature amplitude modulation (QAM) may be found in [1]. Although symmetric signal constellations are optimum for uncoded systems, the same is not necessarily true for TCM. In fact, it has been shown [2,3,4] that by designing the signal constellations to be asymmetric, one can in many instances obtain a performance gain over the traditional symmetric TCM designs.

The measure of performance gain and the amount of it achieved are, in general, functions of many factors, namely, signal-to-noise ratio (SNR), complexity of the trellis encoder (number of trellis code states), and the number of modulation levels (M). For TCM systems, an asymptotic measure of performance gain is the comparison of the minimum free Euclidean distance d_{free} of the trellis code relative to the minimum distance d_{min} of the uncoded modulation. This performance measure is an indication of the maximum reduction in required bit energy-to-noise spectral density ratio E_b/N_0 that can be achieved for arbitrarily small system bit error rates. At practical bit error rate values, this measure can often be misleading since the "real" gain in E_b/N_0 reduction due to coding and possibly asymmetry could be significantly less. More important, however, is the fact that in certain cases of asymmetry, the asymptotic improvement as measured by d_{free} can be achieved in the limit

only as points in the signal constellation merge together, i.e., the trellis code becomes catastrophic. An example of such is the 2-state code which, for all values of n, asymptotically results in 3 dB gain over the same bandwidth uncoded system [3,4].

Here we demonstrate a new and novel trellis coded modulation technique referred to as multiple trellis code modulation (MTCM) (the significance of this acronym will be apparent shortly) which is capable of achieving the above asymptotic performance gains without resorting to modulation asymmetry. As such, this technique circumvents the problem of code catastrophe and other potential problems, e.g., increased phase jitter sensitivity, associated with moving signal points in the constellation arbitrarily close together. The principle behind our discovery is to design a rate nk/(n+1)k (k=2,3,4...) encoder and combine it (again through a suitable mapping function analogous to that employed in [1]) with a 2^{n+1}-point signal constellation outputting k of these signal points (one for each group of (n+1) encoder output symbols) in each transmission interval. Since, in each transmission interval, kn bits enter the encoder and k symbols leave the modulator, the throughput is still n bps/Hz and we again have a unity bandwidth expansion relative to a 2^n-point uncoded system. The surprising thing, however, is that values of k greater than 1 (k=1 corresponds to the conventional TCM system), can, for certain cases, produce increased values of d_{free} with symmetric modulations.

The first part of this report demonstrates this discovery for 2-state trellis diagrams with MPSK and M-AM modulations. In particular, for MPSK, using k=2 when n=1, i.e., rate 1/2 trellis coded QPSK, and using k=4 for n>1, i.e, rate n/(n+1) trellis coded 2^{n+1} - PSK, we are able to achieve the above-mentioned 3 dB asymptotic performance gain improvement using a symmetric

modulation. Also, in the latter case (n>1), we have shown that values of k=2,3 still give performance improvement relative to the conventional (k=1) TCM approach, but by an amount less than the maximum achievable 3 dB.

For M-AM, a value of k=4 for all $n \geq 1$ is required to achieve the maximum performance gain from the multiple trellis coding scheme and a symmetric modulation. In this case, however, we achieve a 3 dB asymptotic gain theoretically only as M approaches infinity (the reason for this will be explained later on). From a practical standpoint, however, a value of M=16 brings us arbitrarily close, i.e., a gain of 2.96 dB. Also, as for MPSK, values of k=2,3 give proportionate gains relative to the conventional TCM approach. These results, including the mapping procedure for achieving the above-mentioned performance gains, will be discussed first.

In the second part of the report, we generalize the above by considering trellises with more than 2 states and also allowing for throughputs whose values are not necessarily integers.

2. 2-State Multiple Trellis Code Modulation

To properly set the stage for the general 2-state case, we begin with two simple examples.

Example #1

Figure 1a is the 2-state trellis diagram for conventional rate 1/2 trellis coded QPSK and Figure 1b is the corresponding multiple trellis diagram for the same coded modulation. In Figure 1b, we have n=1 and k=2 and thus there are $2^{nk} = 4$ branches emanating from each state. Since there are only 2 states in the diagram, this implies that there must be two parallel branches between each pair of states. Also, since k=2, we have two output QPSK symbols* assigned to each branch. The assignment of these symbols to each branch is made to maximize the minimum Euclidean distance between the path through the trellis corresponding to correct reception of the transmitted symbols and that corresponding to an error event path. Also, the assignment must be made in such a way as to prevent the code from becoming catastrophic, i.e., a finite number of channel symbol errors producing an infinite number of decoded bit errors.

Figure 1b illustrates the appropriate assignment of QPSK symbol pairs for each branch in the trellis diagram. Assuming the all zero sequence as the transmitted bit sequence with corresponding all "0" QPSK output symbols, then the error event path of length one, i.e., the parallel path between successive zero states, produces a squared Euclidean distance

$$d^2 = 2d^2(0,2) = 2(4) = 8 \tag{1a}$$

*For convenience, we denote the QPSK symbol s_j simply by its subscript "j" on the branch labels.

where $d^2(i,j)$ denotes the squared Euclidean distance between QPSK symbols s_i and s_j. For the error event path of length two (illustrated by dashed lines in Figure 1b), we see that the squared Euclidean distance is

$$d^2 = d^2(0,0) + d^2(0,2) + d^2(0,1) + d^2(0,3)$$
$$= 0 + 4 + 4\sin^2\phi/2 + 4\cos^2\phi/2 = 8 \qquad (1b)$$

independent of the asymmetry angle ϕ. Thus, we may choose $\phi = \pi/2$ (symmetric QPSK) and obtain a rate 1/2 trellis coded QPSK modulation which achieves a squared free distance equal to 8. We recall that for the conventional TCM of Figure 1a, we can achieve $d^2_{free} = 6$ for the symmetric QPSK constellation and $d^2_{free} = 8$ for the asymmetric constellation whose adjacent signal points merge together, i.e., the code becomes catastrophic [3,4].

Example #2

Figure 2 is the 2-state trellis diagram for conventional rate 1/2 trellis coded 4-AM (note that the output symbols assigned to the transitions emanating from state "1" are reversed with respect to those in Figure 1a so as to get maximum gain from the asymmetry of the modulation [5]). The appropriate trellis diagram for rate 1/2 multiple (k=2 for this example) trellis coding of symmetric 4-AM (distance 2 between adjacent signal points) is identical to Figure 1b with the understanding that the branch assignments now correspond to two 4-AM symbols per branch. Assuming the all "0" 4-AM sequence transmitted, then the error event of length one., i.e., the parallel path between successive zero states, produces a normalized (by the average power of the signal set which, in this case, has value equal to 5) squared Euclidean distance

$$d^2 = \frac{d^2((0,0),(2,2))}{P_{av}} = \frac{2(4)^2}{5} = \frac{32}{5} = 6.4 \qquad (2a)$$

For the error event path of length two, the squared Euclidean distance is given by

$$d^2 = \frac{d^2((0,0),(0,2)) + d^2((2,2),(1,3))}{5} = \frac{(4)^2 + 2(2)^2}{5} = \frac{24}{5} = 4.8 \tag{2b}$$

Thus, the minimum free distance squared is the smaller of (2a) and (2b) namely,

$$d^2_{free} = 4.8 \tag{2c}$$

Relative to the squared minimum distance of uncoded 2-AM (same bandwidth as rate 1/2 trellis coded 4-AM) which has value 4 [5], we achieve a gain of 0.792 dB. We recall that conventional rate 1/2 trellis coded symmetric 4-AM produced no gain relative to the uncoded 2-AM [5]. Thus, even for just k=2, multiple trellis coding has bought us an advantage.

We recall [5] that when asymmetry was introduced into the 4-AM modulation, then asymptotically the squared Euclidean distance achieved by conventional TCM could approach 32/4 = 8.0 or a gain of 3 dB over the uncoded system. Once again to achieve that gain it was necessary to merge signal points together (i.e., s_0 with s_1 and s_2 with s_3) which results in a catastrophic code. Here we will see shortly that with k=4, we can achieve a squared Euclidean distance equal to 32/5 = 6.4 or a gain of 2.041 dB over the uncoded system. For larger values of k, we are limited by the Euclidean distance of the error event path of length one, and thus d_{free} cannot increase beyond the above value.

The reason that we cannot achieve with multiple trellis coding of symmetry M-AM the same maximum gain "achieved" with conventional trellis coding of asymmetric M-AM is explained as follows. We see from the above simple example that, ignoring the normalization by the average power of the

signal set, we can in either case achieve a squared free distance equal to 32. With multiple trellis coding, the signal set remains symmetric and hence the normalization is constant, e.g., a value of 5. When asymmetry is introduced into M-AM modulation, as in Figure 2 for example, the average power is reduced, e.g., to a value of 4 in the limit as adjacent 4-AM signal points merge together. Thus, the difference in performance gain between the two schemes relative to an equivalent bandwidth uncoded system is attributed to the reduction in the average power of the latter. As the number of levels, M, gets larger, the reduction of the average power of the signal set due to asymmetry becomes smaller; thus in the limit of large M, the multiple trellis coded symmetric M-AM will approach the 3 dB gain over the uncoded system. Numerical justification of this discussion will appear later on in Table 2.

A. The General Mapping Procedure for 2-State Multiple Trellis Encoding

As in [1], we begin by partitioning the original signal point constellation into two constellations each with maximum distance among its signal points. This is tantamount to assigning alternate points of the original constellation to each of the two partitions (see Figure 3 for example). Then, the first observation is that signals in partition #1 will be used for transitions emanating from state "0" and signals in partition #2 will be used for transitions emanating from state "1".

From the above discussion of k-multiple trellis coding, we note that there will be 2^{nk-1} parallel paths between like states, e.g., "0" and "0" or "1" and "1", and the same number of parallel paths between unlike states, e.g., "0" and "1" or "1" and "0". For the transition between like states, we assign to each parallel path a sequence of k symbols (we shall refer to this as a k-tuple) all chosen from a fixed partition (of 2^n points)

such that the minimum squared distance between any two of these parallel paths is equal to twice the minimum squared distance between points in the partition, i.e., $8 \sin^2 \pi/2^n$ for MPSK and $32/[(2^{2n+2}-1)/3]$ for M-AM*. The remaining 2^{nk-1} k-tuples formed from symbols in the same partition are assigned to the parallel paths corresponding to a transition to an unlike state. The minimum squared distance among all pairs of parallel paths between unlike states will also be twice the minimum squared distance between points in the partition. However, the minimum squared distance among all pairs of paths consisting of a path between like states and a path between unlike states both originating from the same state is only equal to the minimum squared distance between the points in the partition, i.e., $4 \sin^2 \pi/2^n$ for MPSK and $16/[(2^{2n+2}-1)/3]$ for M-AM. Note that thus far the distances discussed have been independent of the multiplicity k.

The place where the trellis multiplicity k has its influence is in regard to the minimum squared distance among all pairs of paths consisting of a path between like states and one between unlike states where the two paths originate from two different states. With the above k-tuple assignments, this minimum squared distance is k times the minimum squared distance between points in one partition and points in the other, i.e., $4k \sin^2 \pi/2^{n+1}$ for MPSK and $4k/[(2^{2n+2}-1)/3]$ for M-AM. As we shall see in the next section, it is the increase in these distances with k that increases the minimum distance associated with the error event path of length 2 and thus allows for an improvement in d_{free} performance. The examples provided by the trellis diagrams of Figure 4 are further illustrations of the general mapping procedure.

*Herein in our discussion of M-AM distances, we shall assume that the signal point constellation and its partition have been normalized by $P_{av} = (2^{n+2}-1)/3$.

B. Evaluation of Minimum Squared Free Distance

If one constructs a 2-state trellis based upon the above mapping procedure then clearly the minimum squared distance for an error event path of length 1 is the minimum squared distance among parallel paths between like states, i.e., $d_1^2 = 8 \sin^2\pi/2^n$ for MPSK and $32/[(2^{2n+2}-1)/3]$ for M-AM. For the error event path of length 2 (see the dashed curve in Figure 1b for example), the minimum squared distance is made up of two parts. The first part corresponds to the minimum squared distance between two paths originating from the same state one of which terminates in a like state and the other in an unlike state. As discussed above, this is given by $4 \sin^2\pi/2^n$ for MPSK and $16/[(2^{2n+2}-1)/3]$ for M-AM. The second part corresponds to the minimum squared distance between two paths which originate from two different states and both terminate in the same state. Again from the above discussion, this is given by $4k \sin^2\pi/2^{n+1}$ for MPSK and $4k/[(2^{2n+2}-1)/3]$ for M-AM. Thus, the minimum squared distance for the error event path of length 2 is $d_2^2 = 4 \sin^2\pi/2^n + 4k \sin^2\pi/2^{n+1}$ for MPSK and $d_2^2 = (16 + 4k)/[(2^{2n+2}-1)/3]$ for M-AM. Finally, then the minimum squared free distance for the 2-state multiple trellis coding scheme is the smaller of d_1^2 and d_2^2, namely,

$$d_{free}^2 = \min \{8 \sin^2\pi/2^n,\ 4 \sin^2\pi/2^n + 4k \sin^2\pi/2^{n+1}\} \text{ for MPSK}$$

$$d_{free}^2 = \min \{32/[(2^{2n+2}-1)/3],\ (16 + 4k)/[(2^{2n+2}-1)/3]\} \text{ for M-AM} \qquad (3)$$

It is interesting to investigate, as a function of n, the value of trellis multiplicity k which if increased causes d_2^2 to become greater than d_1^2, i.e., the largest value of k beyond which there is no performance improvement in d_{free}. In particular, we seek the largest integer k for which

$d_1^2 > d_2^2$. From the above, using straightforward trigonometric manipulations, we arrive at the result

$$k_{max} = \lceil 2(1 + \cos \pi/2^n) \rceil \leq 4 \quad \text{for MPSK}$$

$$k_{max} = 4 \quad \text{for M-AM} \tag{4}$$

From (4) we see the following interesting results. For MPSK, a value of n = 1 yields $k_{max} = 2$ whereas for any n>1, $k_{max} = 4$. For M-AM, we have $k_{max} = 4$ for all $n \geq 1$.

Tables 1 and 2 tabulate, for MPSK and M-AM respectively, d_{free}^2, as computed from (3), versus n for values of k from 1 to k_{max}. Also tabulated are: 1) the performance gain (in dB) of multiple trellis coded MPSK (M-AM) relative to conventional TCM obtained by taking the ratio of d_{free}^2 for the given value of k to d_{free}^2 for k=1, and 2) the performance gain (in dB) of multiple trellis coded MPSK (M-AM) relative to uncoded symmetric 2^n-MPSK (M-AM).

C. New Description of Multiple Trellis Coding

A few years back, Calderbank and Mazo [6] introduced a new description of conventional trellis codes which expressed the modulator output as a series expansion of products (of all order) of the encoder input bits. The advantages of this new approach were manyfold. First, it was no longer necessary, as in previous discussions, to treat the overall design as a two-step process, i.e., specify an underlying trellis code and then map the output code symbols into the fixed signal constellation based on the "mapping by set partitioning rule" [1]. The new trellis code description given in [6] allowed these two steps to be combined into one. Second, the input/output description of the system afforded by [6] allowed the implementation of the

transmitter to be drawn by inspection. Finally, the representation of [6] was particularly convenient for studying the behavior of trellis coded modulations in an intersymbol interference (ISI) environment.

In [7], the work of Calderbank and Mazo [6] was reviewed and discussed in the context of its application to the optimum design of trellis coded asymmetric modulations. Here, we generalize the work of [6] and [7] to multiple trellis coding.

Let $\{b_i\}$ be a sequence of ± 1-valued real variables which are a mapping of the 0, 1-valued encoder input sequence $\{a_i\}$ according to the linear transformation

$$b_i = 1 - 2a_i \tag{5}$$

Then, for a conventional (k=1) trellis code, the modulator output $x(b_1,b_2,\ldots,b_m)$* may be written as a sum of products of the b_i's [6,7], namely,

$$x(b_1,b_2,\ldots,b_m) = d_0 + \sum_{i=1}^{m} d_i b_i + \sum_{\substack{i,j=1 \\ j>1}}^{m} d_{ij} b_i b_j + \sum_{\substack{i,j,k=1 \\ k>j>i}}^{m} d_{ijk} b_i b_j b_k + \ldots + d_{1\ldots m} b_1 b_2 \ldots b_m \tag{6}$$

where the d's are a set of constraints that can be determined by a simple vector multiplication as follows.

Let $\underline{x} = (x^{(1)},x^{(2)},\ldots,x^{(2^m)})$ denote a column vector of length 2^m whose components represent the 2^m values that $x(b_1,b_2,\ldots,b_m)$ can take on. Next let $\underline{d} = (d_0,d_1,\ldots,d_m,d_{12},d_{13},\ldots,d_{1..m})$ denote a 2^m-length column

*The sequence length m is equal to the sum of n, the number of input bits per channel symbol, and v, the memory of the code (2^v is the number of states of the encoder).

vector of the unknown constants. Finally, let B be a 2^m x 2^m matrix where each row represents the 2^m values taken by all products of the b_i's called for in Eq. (6) for each sequence $b_1, b_2, \ldots, b_m$. In terms of these definitions, Eq. (6) can be written in the matrix form

$$\underline{x} = B\ \underline{d} \tag{7}$$

If $\underline{\beta}$ is a vector corresponding to a particular product of the b_i's (i.e., a column of B), then as shown in [6,7], the corresponding coefficient of that product in the expansion of Eq. (6) is simply obtained from

$$d = \frac{1}{2^m}\ \underline{\beta}^T \underline{x} \tag{8}$$

i.e., the Hadamard transform of the vector $\underline{x}$. In (8), the "T" superscript denotes the transpose operation.

To apply this description to <u>multiple</u> trellis coding, we simply note that a description such as Eq. (6) is appropriate for each of the k elements in the k-tuples assigned to the trellis branches. Thus, letting $\underline{x}^{(i)}$; i = 1,2,...,k denote the <u>i</u>th modulator output corresponding to an input sequence of length nk, then the matrix representation of (7) is appropriate to $\underline{x}^{(i)}$ and yields a vector $\underline{d}^{(i)}$ in accordance with (8). The set of vectors $\{\underline{d}^{(i)}\}$; i = 1,2,...,k determined as above completely describes the multiple trellis code.

<u>Example #1</u>

As a simple example of the above, consider the case of rate 1/2 (n=1) multiple (k=2) trellis coded 4-AM with memory v=1 (2 states). The

length of the input sequence upon which each output symbol $x^{(i)}$; i = 1,2 depends is now m = nk + v = 3. For m=3, Eq. (6) simplifies to*

$$x(b_1,b_2,b_3) = d_1b_1 + d_2b_2 + d_3b_3 + d_{12}b_1b_2 + d_{13}b_1b_3 + d_{23}b_2b_3 + d_{123}b_1b_2b_3 \quad (9)$$

Here b_3 denotes the previous state and b_1 the present state. (Note that neither the previous nor the present state depend on b_2. Rather b_2 is used to decide between the parallel paths between states.) From the trellis diagram of Figure 1b (with state "0" and "1" respectively replaced by "1" and "-1" in accordance with Eq. (5) and the signal constellation of Figure 2 (with $\Delta = 0$) we have

$$\begin{aligned}
x^{(1)}(1,1,1) &= -3 & x^{(2)}(1,1,1) &= -3 \\
x^{(1)}(1,-1,1) &= 1 & x^{(2)}(1,-1,1) &= 1 \\
x^{(1)}(-1,1,1) &= -3 & x^{(2)}(-1,1,1) &= 1 \\
x^{(1)}(-1,-1,1) &= 1 & x^{(2)}(-1,-1,1) &= -3 \\
x^{(1)}(-1,1,-1) &= -1 & x^{(2)}(-1,1,-1) &= -1 \\
x^{(1)}(-1,-1,-1) &= 3 & x^{(2)}(-1,-1,-1) &= 3 \\
x^{(1)}(1,1,-1) &= -1 & x^{(2)}(1,1,-1) &= 3 \\
x^{(1)}(1,-1,-1) &= 3 & x^{(2)}(1,-1,-1) &= -1
\end{aligned} \quad (10)$$

Then, using Eq. (10), the expansion of Eq. (6) can be put in the matrix form of Eq. (7) where

*As in [6], we choose the additive constant $d_0 = 0$ with no loss in generality. This assumption reduces the dimensionality of $\underline{d}$ and B to $2^m - 1$ and $2^m \times 2^m - 1$, respectively.

$$\underline{x}^{(1)} = \begin{bmatrix} -3 \\ 1 \\ -3 \\ 1 \\ -1 \\ 3 \\ -1 \\ 3 \end{bmatrix} \quad ; \quad x^{(2)} = \begin{bmatrix} -3 \\ 1 \\ 1 \\ -3 \\ -1 \\ 3 \\ 3 \\ -1 \end{bmatrix} \quad ; \quad \underline{d} = \begin{bmatrix} d_1 \\ d_2 \\ d_3 \\ d_{12} \\ d_{13} \\ d_{23} \\ d_{123} \end{bmatrix} \tag{11}$$

and

$$B = \begin{bmatrix} b_1 & b_2 & b_3 & b_1b_2 & b_1b_3 & b_2b_3 & b_1b_2b_3 \\ 1 & 1 & 1 & 1 & 1 & 1 & 1 \\ 1 & -1 & 1 & -1 & 1 & -1 & -1 \\ -1 & 1 & 1 & -1 & -1 & 1 & -1 \\ -1 & -1 & 1 & 1 & -1 & -1 & 1 \\ -1 & 1 & -1 & -1 & 1 & -1 & 1 \\ -1 & -1 & -1 & 1 & 1 & 1 & -1 \\ 1 & 1 & -1 & 1 & -1 & -1 & -1 \\ 1 & -1 & -1 & -1 & -1 & 1 & 1 \end{bmatrix} \tag{12}$$

To solve for the elements of $\underline{d}^{(i)}$; i = 1,2, we make use of Eq. (8). For example, using the second and third columns of B for $\underline{d}^{(1)}$ and the third and seventh columns of B for $\underline{d}^{(2)}$ we would have

$$d_2^{(1)} = \frac{1}{8}\begin{bmatrix} 1 & -1 & 1 & -1 & 1 & -1 & 1 & -1 \end{bmatrix}\begin{bmatrix} -3 \\ 1 \\ -3 \\ 1 \\ -1 \\ 3 \\ -1 \\ 3 \end{bmatrix} = -2 \qquad d_3^{(1)} = \frac{1}{8}\begin{bmatrix} 1 & 1 & 1 & 1 & -1 & -1 & -1 & -1 \end{bmatrix}\begin{bmatrix} -3 \\ 1 \\ -3 \\ 1 \\ -1 \\ 3 \\ -1 \\ 3 \end{bmatrix} = -1$$

$$d_3^{(2)} = \frac{1}{8}\begin{bmatrix} 1 & 1 & 1 & 1 & -1 & -1 & -1 & -1 \end{bmatrix}\begin{bmatrix} -3 \\ 1 \\ 1 \\ -3 \\ -1 \\ 3 \\ 3 \\ -1 \end{bmatrix} = -1 \qquad d_{123}^{(2)} = \frac{1}{8}\begin{bmatrix} 1 & -1 & -1 & 1 & 1 & -1 & -1 & 1 \end{bmatrix}\begin{bmatrix} -3 \\ 1 \\ 1 \\ -3 \\ -1 \\ 3 \\ 3 \\ -1 \end{bmatrix} = -2$$

(13)

Application of Eq. (8) to the remaining columns of B results in zero values for all other d's. Thus, the trellis of Figure 1b is represented by the relations

$$x^{(1)} = -2b_2 - b_3$$
$$x^{(2)} = -b_3 - 2b_1b_2b_3 \qquad (14)$$

A simple implementation of Eq. (14) as a transmitter is illustrated in Figure 5. Note that Figure 5 represents the combined modulation/coding process without the necessity of separating it into its component parts, i.e., a trellis code followed by a rule for mapping and an AM modulator.

Example #2

As a second example, consider the case of rate 1/2 (n=1) multiple (k=2) trellis coded QPSK with memory v=1. Since once again m=3, Eq. (9) holds for the input/output relationship of the trellis encoder. Here, however, the output symbol, x, represents phase instead of amplitude and the true encoder output, y, is given (in complex notation) by $y = e^{jx}$ [7]. Similarly, the trellis diagram of Figure 1b is appropriate together with the signal constellation of Figure 1a (with $\phi = 0$). In particular,

$$\begin{aligned}
x^{(1)}(1,1,1) &= -\pi/4 & x^{(2)}(1,1,1) &= -\pi/4 \\
x^{(1)}(1,-1,1) &= 3\pi/4 & x^{(2)}(1,-1,1) &= 3\pi/4 \\
x^{(1)}(-1,1,1) &= -\pi/4 & x^{(2)}(-1,1,1) &= 3\pi/4 \\
x^{(1)}(-1,-1,1) &= 3\pi/4 & x^{(2)}(-1,-1,1) &= -\pi/4 \\
x^{(1)}(-1,1,-1) &= \pi/4 & x^{(2)}(-1,1,-1) &= \pi/4 \\
x^{(1)}(-1,-1,-1) &= -3\pi/4 & x^{(2)}(-1,-1,-1) &= -3\pi/4 \\
x^{(1)}(1,1,-1) &= \pi/4 & x^{(2)}(1,1,-1) &= -3\pi/4 \\
x^{(1)}(1,-1,-1) &= -3\pi/4 & x^{(2)}(1,-1,-1) &= \pi/4
\end{aligned} \qquad (15)$$

Putting Eq. (15) in vector form as in Eq. (11), then using Eq. (12) and solving for $\underline{d}^{(i)}$; i=1,2 from Eq. (8) gives the desired result, namely,

$$x^{(1)} = \frac{\pi}{4}(b_3 - 2b_2b_3)$$

$$x^{(2)} = \frac{\pi}{4}(b_3 - 2b_1b_2) \tag{16}$$

Figure 6 is an implementation of Eq. (16) where the phase modulator is used to convert x to y in accordance with the relation given above.

D. Bit Error Probability Performance

Thus far our entire discussion has focussed on performance gain as measured by improvement in minimum free distance of the trellis code. In the limit as the system bit error probability becomes arbitrarily small, this measure is equivalent to the improvement in required bit energy-to-noise spectral density ratio. From a more practical standpoint, one is often interested in the reduction of bit energy-to-noise spectral density ratio for a given average bit error probability. Previous results [2-5] on conventional trellis coding showed that such reductions were possible. Using pair-state diagrams and upper bounds on bit error probability computed from the transfer function of these diagrams [2-5], we shall now determine the magnitude of these performance gains for multiple trellis codes.

Without going into great detail, it has been shown [4] that a tight upper bound* on the bit error probability of trellis codes is given by

$$P_b \leq \frac{1}{2n}\,\mathrm{erfc}\left(\sqrt{\frac{nE_b}{N_0}\,\frac{d_{free}^2}{4}}\right) D^{-d_{free}^2}\,\frac{d}{dz}\,T(D,z)\Big|_{z=1} \tag{17}$$

*This bound was shown in [4] to be an excellent match to numerical results obtained by computer simulation.

where erfc x is the complementary error function, D is the Bhattacharyya distance defined by

$$D = \exp\left(-\frac{nE_b}{4N_0}\right) \tag{18}$$

with E_b/N_0 denoting the bit energy-to-noise spectral density ratio, and d^2_{free} is, as before, the squared free distance of the trellis code, and T(D,z) is the transfer function of its pair-state diagram. Provided that one finds the proper pair-state diagram for multiple trellis codes, then Eq. (17) also applies in this case except that the factor of 1/2n is replaced by 1/2nk. We also note that the Bhattacharyya distance for multiple trellis codes is still given by (17) independent of the value of k.

As an example consider a rate 1/2 multiple (k=2) trellis coded QPSK system with trellis diagram as in Figure 1b. The corresponding state diagram is illustrated in Figure 7 and the equivalent pair-state diagram [3] for computing T(D,z) is shown in Figure 8. In Figure 7 the branches are labelled with the input bit and output QPSK symbol pairs that cause that particular transition whereas in Figure 8 the branches are labelled with a gain of the form

$$G = \frac{1}{2nk} z^{\Omega} D^{\delta^2} \tag{19}$$

Here z is an index, Ω is the Hamming distance between input bit sequences and δ^2 is the squared Euclidean distance between MPSK output symbols for the transition between the pair states.

The transfer function of Figure 8 is easily computed as [3]

$$T(D,z) = \frac{(2z + 2z^2 + z^3)D^8 - (z^2 + z^3)D^{12}}{1 - (z + z^2)D^4} \tag{20}$$

where, in accordance with (19),

$$a = \frac{1}{2}(z + z^2)D^4$$

$$b = \frac{1}{2}(1 + z)D^4$$

$$c = \frac{1}{2} zD^8 \tag{21}$$

Substituting (21) into (20) and performing the differentiation required in (17) yields the desired upper bound on P_b, namely,

$$P_b \leq \frac{1}{4} \operatorname{erfc}\left(\sqrt{\frac{2E_b}{N_0}}\right) \times \left(\frac{9 - 8D^4 + 4D^8}{(1 - 2D^4)^2}\right) \tag{22}$$

Figure 9 is an illustration of the upper bound of Eq. (22). Also shown in this figure, for purpose of comparison, are the upper bounds on P_b for uncoded PSK and conventional (k=1) rate 1/2 trellis coded symmetric and optimum* asymmetric QPSK modulations. These results are obtained from [4] in accordance with the relations

$$P_b = \frac{1}{2} \operatorname{erfc}\sqrt{\frac{E_b}{N_0}} \qquad \text{(uncoded PSK)} \tag{23}$$

$$P_b \leq \frac{\frac{1}{2} \operatorname{erfc}\sqrt{\frac{3E_b}{2N_0}}}{(1 - \exp(-E_b/2N_0))^2} \qquad \text{(coded symmetric)} \tag{24}$$

and

$$P_b \leq \frac{\frac{1}{2} \operatorname{erfc}\left(\sqrt{\frac{E_b}{N_0}\frac{(1+2\alpha)}{(1+\alpha)}}\right)}{(1 - \exp(-E_b/[N_0(1+\alpha)]))^2}$$

(coded optimum asymmetric) (25)

*The value of asymmetry as given in (26) is exactly optimum for a slightly looser upper bound (see [3]) but only approximately optimum for (25).

with

$$\alpha = \frac{E_b/N_0}{\ell n\ 3} - 1 \tag{26}$$

We observe from these results that, over the range of E_b/N_0 illustrated, the multiple trellis scheme is slightly better in performance than the conventional trellis code with optimum asymmetry.

3. Generalized Multiple Trellis Coded Modulation

As mentioned in the introduction, here we generalize the results of Section 2 by considering trellises with more than 2 states and also allowing for throughputs whose values are not necessarily integers. In particular, we propose an encoder with b binary input bits and s binary output symbols which are mapped into k M-ary symbols in each transmission interval (see Figure 10). For such a transmitter, the throughput is b/k bps/Hz which depending on the choice of b and k may or may not be integer-valued.

To produce such a result, we partition the s binary encoder output symbols into k groups of $m = \log_2 M$ symbols each. Each of these groups results in an M-ary modulator output symbol. Thus, the only constraint on the transmitter parameters is that s, k, and M must be chosen such that

$$s = k \log_2 M \tag{27}$$

Furthermore, b is not required to be an integer multiple of the multiplicity k and thus the trellis code rate b/s is not constrained to be the ratio of adjacent integers.

It is interesting to note that the non-integer throughput MTCM's do not have equivalent uncoded counterparts. Thus, in these cases, the notion of unity bandwidth expansion of the trellis coded scheme relative to the uncoded

scheme has no meaning. Instead, we must define a performance measure which directly characterizes the generalized MTCM technique. For this purpose, we shall use the computational cutoff rate R_0 [8] of the channel as a basis for demonstrating the efficiency of the above technique (in terms of the required bit energy-to-noise ratio at a sufficiently small error rate). This procedure is analogous to but simpler than that performed by Ungerboeck [1] who used channel capacity as his basis of comparison.

A. Computational Cutoff Rate for Generalized MTCM Channels

The computational cutoff rate is dependent only on the coding channel and not on the coding scheme. For MPSK modulation, and discrete memoryless channels, R_0 is given by

$$R_0 = \log_2 M - \log_2\left[1 + \sum_{i=1}^{M-1} D^{4\sin^2(i\pi/M)}\right] \tag{28}$$

where D is again the Bhattacharyya distance that depends only on the decoder metric. In our case, i.e., a maximum-likelihood metric, D is given by

$$D = \exp\left(-\frac{E_s}{4N_0}\right) \tag{29}$$

where E_s is the energy of an M-ary channel symbol. For generalized MTCM, E_s is related to the input bit energy by $E_s = (b/k)E_b$. For the simple MTCM case discussed in Section 2 where $b/k = n$, (29) becomes (18), which is independent of multiplicity and thus also characterizes conventional TCM.

B. Error Probability Performance

Analogous to (17), an upper bound on the bit error probability performance of generalized MTCM is given by

$$P_b \leq \frac{1}{2b}\,\mathrm{erfc}\left(\sqrt{\frac{bE_b}{kN_0}\,\frac{d_{free}^2}{4}}\right) D^{-d_{free}^2}\,\frac{d}{dz}\,T(D,z)\Big|_{z=1} \tag{30}$$

Similarly, an upper bound on first error event probability P_e [9] is given by

$$P_e \leq \frac{1}{2}\,\mathrm{erfc}\left(\sqrt{\frac{bE_b}{kN_0}\,\frac{d_{free}^2}{4}}\right) D^{-d_{free}^2}\,T(D) \tag{31}$$

Both of these bounds require determining the transfer function of the pair state diagram [9] associated with the trellis. For trellises with large numbers of states, this process can become analytically quite cumbersome. Thus, instead we consider an approximate (asymptotically approached at high SNR) lower bound which for first error event probability is given by

$$P_e \leq \frac{1}{2}\,\mathrm{erfc}\left(\sqrt{\frac{bE_b}{kN_0}\,\frac{d_{free}^2}{4}}\right) \times N(d_{free}) \tag{32}$$

where $N(d_{free})$ is the number of error event paths at distance d_{free} from the all zeros path, i.e., the multiplicity of error events at distance d_{free}. In effect, (32) represents the result that would be obtained from (31) by keeping only the first term in the power series expansion of T(D).

The approximate lower bound of (32) can be simplified (at a slight expense in tightness) still further by ignoring $N(d_{free})$. Thus, for a given P_e, e.g., 10^{-6}, we can readily compute the required E_b/N_0 for any particular generalized MTCM with given values of b, k, and M once we determine its d_{free}.

Next, we give several examples illustrating the procedure and then examine their communication efficiency relative to R_0.

Example 1

Consider a trellis encoder with b=3, s=6, whose binary output symbols are mapped into 8PSK symbols with multiplicity k=2 in accordance with (27). The throughput of this MTCM scheme is thus b/k = 1.5 bps/Hz. We again note that there is no equivalent (same throughput) uncoded modulation. In fact, the above MTCM scheme is exactly midway between BPSK with a throughput of 1 bps/Hz and QPSK with a throughput of 2 bps/Hz. For the above example, the number of transitions emanating from each state in the trellis diagram is $2^b = 8$. If we postulate that there are to be no parallel paths between transitions (later examples will relax this requirement), then the minimum number of states for the trellis must be 8, i.e., a fully-connected trellis. Thus, we begin by considering this specific case.

1. 8-State Trellis

In accordance with the above, we must assign a pair (k=2) of 8PSK symbols to each trellis branch in such a way as to maximize the free distance of the code. For the symmetric 8PSK signal set illustrated in Figure 11, define the sets (pairs of 8PSK symbols)*

$$\begin{array}{llll} A_0 = 0\ 0 & A_4 = 2\ 2 & B_0 = 0\ 2 & B_4 = 2\ 0 \\ A_1 = 4\ 4 & A_5 = 6\ 6 & B_1 = 4\ 6 & B_5 = 6\ 4 \\ A_2 = 0\ 4 & A_6 = 2\ 6 & B_2 = 0\ 6 & B_6 = 2\ 4 \\ A_3 = 4\ 0 & A_7 = 6\ 2 & B_3 = 4\ 2 & B_7 = 6\ 0 \end{array} \qquad (33)$$

*For simplicity, we denote the MPSK symbol merely by its subscript.

These sets have the following minimum squared Euclidean distances:

$$\begin{aligned} d^2_{min}\ (A_i,A_j) &= 4 \\ d^2_{min}\ (B_i,B_j) &= 4 \\ d^2_{min}\ (A_i,B_j) &= 2 \end{aligned} \tag{34}$$

We assign the A_i's to the paths leaving the odd-numbered states each time permuting the assignment by one. Similarly, we assign the B_i's to the paths leaving the even-numbered states with the same permutation (see Figure 12). When this is done, the minimum distance path will be of length 2 (see Figure 12) and thus the squared free distance for the code is

$$d^2_{free} = d^2_{min}\ (A_i,A_j) + d^2_{min}\ (A_i,B_j) = 4 + 2 = 6 \tag{35}$$

Note that, in effect, we require only a QPSK signalling set to achieve the above. We remind the reader that conventional rate 1/2 trellis coded QPSK (throughput = 1 bps/Hz) with an 8 state trellis resulted in $d^2_{free} = 12.0$ whereas conventional rate 2/3 trellis coded 8PSK (throughput = 2 bps/Hz) with an 8 state trellis produced $d^2_{free} = 6 - \sqrt{2} = 4.586$ [3].

2. 16-State Trellis

Here we still assume no parallel paths between states but use a half-connected trellis (each state transitions to only half the total number of states). The trelliis and multiple 8PSK symbol set assignment are illustrated in Figure 13. In particular, we do as before, namely, we assign the A_i's to the paths leaving the odd-number states and the B_i's to the paths leaving the even-numbered states. With the assignment of Figure 13, the minimum distance path is of length 2 and

$$d^2_{free} = d^2_{min}(A_i, A_j) + d^2_{min}(A_i, A_j) = 4 + 4 \qquad (36)$$
$$= 8$$

This is to be compared with values of $d^2_{free} = 14$ and $d^2_{free} = 5.172$ for 16-state conventional rate 1/2 trellis coded QPSK and rate 2/3 trellis coded 8PSK respectively. Again, we note that, in effect, only QPSK signalling is used.

Example 2

The free distance of the MTCM schemes of Example 1 can be increased by defining the mapping sets such that transitions between states contain parallel paths. In particular, we define sets containing 2 elements per set as follows:

$$C_0 = \begin{cases} 00 \\ 44 \end{cases} \qquad E_0 = \begin{cases} 11 \\ 55 \end{cases}$$

$$C_1 = \begin{cases} 04 \\ 40 \end{cases} \qquad E_1 = \begin{cases} 15 \\ 51 \end{cases}$$

$$C_2 = \begin{cases} 22 \\ 66 \end{cases} \qquad E_2 = \begin{cases} 33 \\ 77 \end{cases}$$

$$C_3 = \begin{cases} 26 \\ 62 \end{cases} \qquad E_3 = \begin{cases} 37 \\ 73 \end{cases}$$

$$D_0 = \begin{cases} 02 \\ 46 \end{cases} \qquad F_0 = \begin{cases} 13 \\ 57 \end{cases}$$

$$D_1 = \begin{cases} 06 \\ 42 \end{cases} \qquad F_1 = \begin{cases} 17 \\ 53 \end{cases}$$

$$D_2 = \begin{cases} 20 \\ 64 \end{cases} \qquad F_2 = \begin{cases} 31 \\ 75 \end{cases}$$

$$D_3 = \begin{cases} 24 \\ 60 \end{cases} \qquad F_3 = \begin{cases} 35 \\ 71 \end{cases} \qquad (37)$$

These sets have the following squared Euclidean distances:

$$
\begin{aligned}
&d^2(C_i) = 8 && d^2(E_i) = 8 \\
&d^2(C_i,C_j)\Big|_{i\neq j} = 4 && d^2(E_i,E_j)\Big|_{i\neq j} = 4 \\
&d^2_{min}(C_i,D_j) = 2 && d^2_{min}(E_i,F_j) = 2 \\
&d^2(D_i) = 8 && d^2(F_i) = 8 \\
&d^2(D_i,D_j)\Big|_{i\neq j} = 4 && d^2(F_i,F_j)\Big|_{i\neq j} = 4
\end{aligned}
\qquad (38)
$$

where $d^2(X_i)$ is the squared Euclidean distance between the two elements in the set, $d^2(X_i,Y_j)$ is the squared Euclidean distance between either element in X_i and either element in Y_j, and $d^2_{min}(X_i,Y_j)$ is the minimum of the squared Euclidean distances between either element in X_i and either element in Y_j.

Since b = 3 (2^b = 8 paths emanating from a given state) and there are two parallel paths per transition (i.e., each corresponding to one of the two elements in a given set), then each state will now have a transition to only 4 other states. We begin by considering a trellis with 4 states which implies a fully connected trellis.

1. 4-State Trellis

Consider the trellis of Figure 14 where the C_i sets have been assigned to the paths leaving states 1 and 3 and the D_i sets have been assigned to the paths leaving states 2 and 4. Again we permute the assignment by one between paths leaving state 1 and paths leaving state 3, and similarly for states 2 and 4. By inspection of Figure 14, we immediately find that the minimum distance path is of length 2 with squared Euclidean distance

$$d^2(C_i,C_j)\Big|_{i\neq j} + d^2_{min}(C_i,D_j) = 4 + 2 = 6 \qquad (39)$$

Since this squared distance is smaller than the squared distance between parallel paths, i.e., $d^2 = 8$, then $d^2_{free} = 6$. We note that by using parallel paths between transitions, we are able to achieve a larger free distance with only 4 states than we achieved previously in Example 1 using 8 states. Also, the set assignment in Figure 14 does not require the use of the E_i and F_i sets. Thus, in effect, we require only a QPSK signalling set to achieve the above.

2. 8-State Trellis

Here we have a half-connected trellis as illustrated in Figure 15 with the C_i's assigned to the odd-numbered states and the D_i's assigned to the even-numbered states. Again the minimum distance path is of length 2 and achieves

$$d^2(C_i,C_j)\Big|_{i\neq j} + d^2(C_i,C_j)\Big|_{i\neq j} = 4 + 4 = 8 \qquad (40)$$

Since this is identical to the squared distance between parallel paths, we have $d^2_{free} = 8$ which is the same as that achieved with 16 states and no parallel paths in Example 1. Again, only a QPSK signalling set is needed since sets E_i and F_i are not assigned to the trellis.

Since the maximum free distance achievable is limited to the distance between parallel paths, we cannot achieve any further improvement by going to 16 states.

Example 3

Consider next a trellis encoder with b=7, s=12, whose binary output symbols are mapped into 8PSK with multiplicity k=4 in accordance with (27). The throughput of this MTCM scheme is b/k = 1.75 with no equivalent uncoded system. There are now 2^b = 128 transitions emanating from each state so that for any number of trellis states less than 128, we must have parallel paths between states. The first case we consider is again that of a fully-connected 8-state trellis which implies that the number of parallel paths between states is 128/8 = 16.

1. 8-State Trellis

In accordance with the above we must assign 16 4-tuples of 8PSK symbols to each trellis branch in such a way as to maximize the free distance of the code. We can use the trellis diagram of Figure 12 but first we must define and then assign the sets of 8PSK 4-tuples. The construction of these sets is as follows:

	Set	Number of Elements Per Set
1)	$A_0 = \begin{cases} 0\ 0\ 0\ 0 \\ 4\ 4\ 4\ 4 \end{cases}$	2
2)	$A_1 = A_0 + 0\ 0\ 4\ 4$	2
	$A_2 = A_0 + 0\ 4\ 0\ 4$	
	$A_3 = A_0 + 4\ 0\ 0\ 4$	
3)	$B_0 = A_0 \cup A_1 \cup A_2 \cup A_3$	8
4)	$B_1 = B_0 + 2\ 2\ 2\ 2$	8

	Set	Number of Elements Per Set	
5)	$C_0 = B_0 \cup B_1$	16	
6)	$C_1 = C_0 + 0\ 0\ 0\ 4$	16	
	$C_2 = C_0 + 0\ 0\ 2\ 2$		
	$C_3 = C_0 + 2\ 2\ 0\ 0$		
	$C_4 = C_0 + 2\ 0\ 0\ 2$		
	$C_5 = C_0 + 2\ 0\ 2\ 0$		
	$C_6 = C_0 + 0\ 2\ 2\ 0$		
	$C_7 = C_0 + 0\ 2\ 0\ 2$		
7)	$D_i = C_i + 0\ 0\ 0\ 2$; $i = 0,1,2,\ldots,7$	16	
8)	$E_i = C_i + 1\ 1\ 1\ 1$; $i = 0,1,2,\ldots,7$	16	
	$F_i = D_i + 1\ 1\ 1\ 1$; $i = 0,1,2,\ldots,7$	16	(41)

Only the final sets, i.e., C_i, D_i, E_i, and F_i, with 16 4-tuples each, are of interest insofar as assignment to the trellis. These sets have the following squared Euclidean distances:

$$d^2_{min}(C_i) = d^2_{min}(E_i) = 8; \quad i = 0,1,2,\ldots,7$$

$$d^2_{min}(C_i,C_j)\Big|_{i\neq j} = d^2_{min}(E_i,E_j)\Big|_{i\neq j} = 4 \tag{42}$$

$$d^2_{min}(C_i,E_j) = 4(2 - \sqrt{2}) \ ; \quad i = 0,1,2,\ldots,7, \ j = 0,1,2,\ldots,7$$

where $d^2_{min}(X_i)$ is the minimum squared Euclidean distance between elements (4-tuples) in the set X_i, and $d^2_{min}(X_i,Y_j)$ is the minimum squared Euclidean distance between any element in X_i and any element in Y_j.

If we replace the trellis branch assignments A_i and B_i of Figure 12 with C_i and E_i, respectively, then, since the distance between parallel branches is 8, the free distance is determined by the minimum distance path of length 2, namely,

$$d^2_{free} = d^2_{min}(C_i,C_j)\Big|_{i\neq j} + d^2_{min}(E_i,E_j)\Big|_{i\neq j}$$
$$= 4 + 4(2 - \sqrt{2}) = 6.343 \tag{43}$$

2. 16-State Trellis

Using the half-connected trellis of Figure 13 and again replacing the A_i and B_i branch assignments with C_i and E_i, respectively, the minimum distance path of length 2 has a squared Euclidean distance

$$d^2 = d^2_{min}(C_i,C_j)\Big|_{i\neq j} = d^2_{min}(C_i,C_j) + d^2_{min}(C_i,C_j)\Big|_{i\neq j}$$
$$= 4 + 4 = 8 \tag{44}$$

Since (44) is equal to the minimum squared distance between parallel paths (i.e., 8), then the squared free distance of the trellis is

$$d^2_{free} = 8 \tag{45}$$

Example 4

As a last example, we consider b = 6, k = 4 and a 4-state trellis. This example has the same throughput as Examples 1 and 2, namely, b/k = 1.5 but with an increase in multiplicity from 2 to 4. The appropriate trellis diagram is illustrated in Figure 16. Here, the even-numbered C_i sets of (41) are assigned to the paths leaving states 1 and 3 while the odd-numbered C_i sets are assigned to the paths leaving states 2 and 4. The minimum distance path is of length 2 and achieves

$$d^2(C_i,C_j)\Big|_{i\neq j} + d^2(C_i,C_j)\Big|_{i\neq j} = 4 + 4 = 8 \qquad (46)$$

which is equal to the squared distance between parallel paths. Thus, $d^2_{free} = 8$. Hence, we can achieve with 4 states and multiplicity 4 the equivalent performance to what required 8 states when the multiplicity was only 2 (see Example 2). Once again going to a larger number of states will result in no gain, since a free distance equal to the distance between parallel paths has already been achieved.

Illustrated in Figure 17 is a plot of R_0 versus E_s/N_0 with M as a parameter as computed from (28) and (29). Superimposed on these curves are points, corresponding to the various examples given in this report, whose abscissa is the required E_s/N_0 to achieve the upper bound on P_e (ignoring the factor $N(d_{free})$) equal to 10^{-6}. The ordinate of these points is obtained by setting $R_0 = b/k$ for each case at hand.

4. Conclusion

Multiple trellis coding, wherein more than one channel symbol per trellis branch is transmitted, has been shown to yield a performance gain with symmetric signal sets comparable to that previously achieved only with signal constellation asymmetry. The advantage of multiple trellis coding over the conventional trellis coded asymmetric modulation technique is that the potential for code catastrophe associated with the latter has been eliminated with no additional cost in complexity (as measured by the number of states in the trellis diagram). While indeed additional computations per branch are needed for the multiple trellis coding scheme, this is thought to be a small price to be paid for the relatively large performance gains achievable.

Also, extension to higher dimensional modulations such as quadrature amplitude modulation (QAM) is obvious from the results of [1] and

[5]. In particular, each pair of M-AM symbols per branch (assuming k is even) would be regarded as the coordinates of a QAM symbol.

References

[1] G. Ungerboeck, "Channel Coding with Multilevel/Phase Signals," IEEE Transactions on Information Theory, Vol. IT-28, No. 1, January 1982, pp. 55-67.

[2] D. Divsalar, and J.H. Yuen, "Asymmetric MPSK for Trellis Codes," GLOBECOM '84 Proceedings, Atlanta, GA, November 26-29, 1984. pp. 20.6.1-20.6.8.

[3] M.K. Simon, and D. Divsalar, "Combined Trellis Coding with Asymmetric MPSK Modulation," JPL Publication 85-24, Pasadena, CA, May 1, 1985.

[4] D. Divsalar, M.K. Simon, and J.H. Yuen, "Trellis Coding with Asymmetric Modulations," accepted for publication in the IEEE Transactions on Communications.

[5] D. Divsalar, D., and M.K. Simon, "Combined Trellis Coding with Asymmetric Modulations," GLOBECOM '85 Proceedings, New Orleans, LA, December, 1985, pp. 21.2.1-21.2.7.

[6] R. Calderbank, and J.E. Mazo, "A New Description of Trellis Codes," IEEE Transactions on Information Theory, Vol. IT-30, No. 6, November, 1984, p. 784-791.

[7] M.K. Simon, and D. Divsalar, "A New Description of Combined Trellis Coding with Asymmetric Modulation," JPL Publication 85-45, Pasadena, CA, July 15, 1985.

[8] J.L. Massey, "Coding and Modulation in Digital Communications," Proc. 1974 Int. Zurich Seminar on Digital Comm., Zurich, Switzerland, March 1974, pp. E2(1)-(4).

[9] A.J. Viterbi, and J.K. Omura, Principles of Digital Communication and Coding, McGraw-Hill Co., New York, NY, 1979.

Table 1. Minimum Squared Free Distance Performance of Multiple Trellis Coded MPSK - 2 States.

d^2_{free}	n	k	Performance Gain Relative to Conventional TCM (k=1)	Performance Gain Relative to Uncoded 2^n-PSK
6.0	1	1	0.0 dB	1.76 dB
8.0	1	2	1.25	3.01
2.586	2	1	0.0	1.116
3.172	2	2	0.887	2.003
3.757	2	3	1.623	2.739
4.0	2	4	1.895	3.01
0.738	3	1	0.0	1.00
0.8903	3	2	0.814	1.814
1.0425	3	3	1.50	2.50
1.172	3	4	2.01	3.01

Table 2. Minimum Squared Free Distance Performance of Multiple Trellis Coded M-AM - 2 States.

d^2_{free}	n	k	Performance Gain Relative to Conventional TCM (k=1)	Performance Gain Relative to Uncoded 2^n-AM
4.0	1	1	0.0 dB	0.0 dB
4.8	1	2	0.792	0.792
5.6	1	3	1.461	1.461
6.4	1	4	2.041	2.041
20/21	2	1	0.0	0.757
24/21	2	2	0.792	1.549
28/21	2	3	1.461	2.218
32/21	2	4	2.041	2.798
20/85	3	1	0.0	0.918
24/85	3	2	0.792	1.71
28/85	3	3	1.461	2.379
32/85	3	4	2.041	2.959

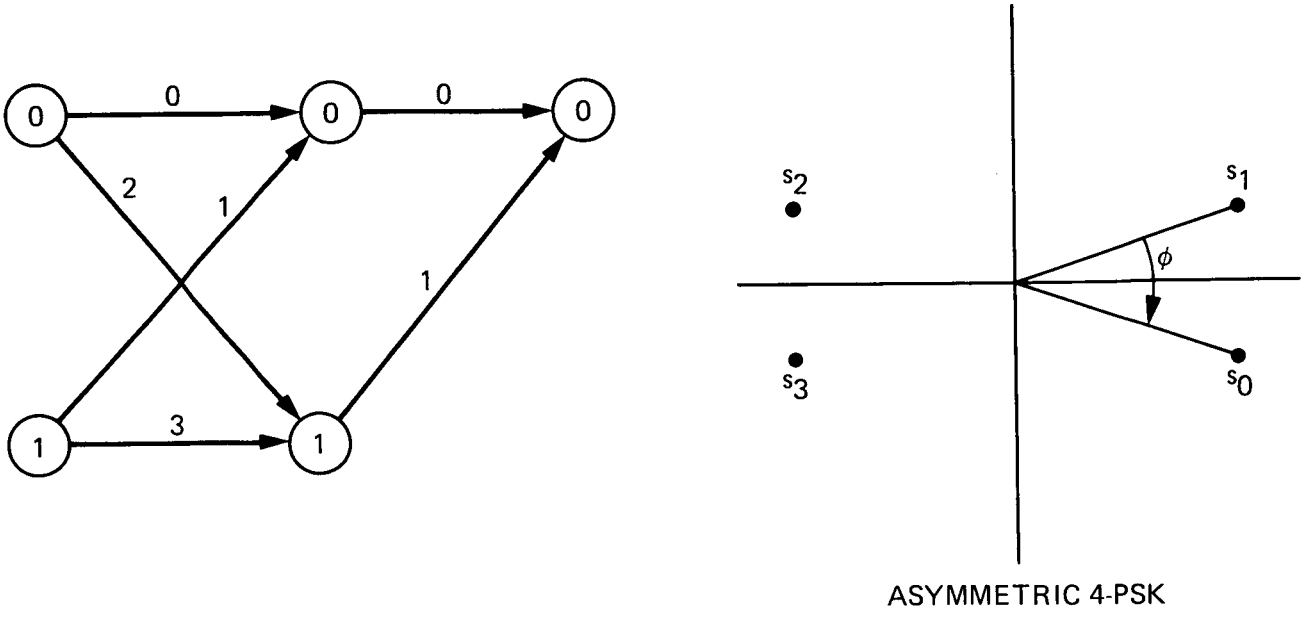

Figure 1a. Trellis Diagram for Conventional Rate 1/2 Trellis Coded QPSK.

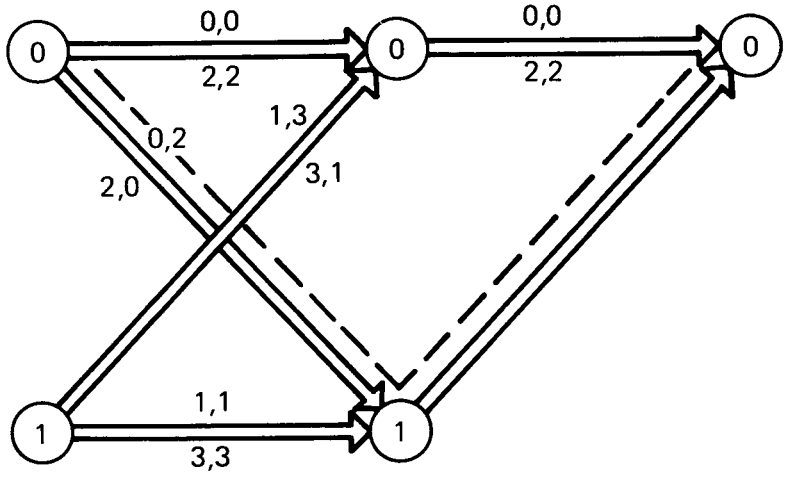

Figure 1b. Trellis Diagram for Rate 1/2 Multiple Trellis Coded QPSK; k=2.

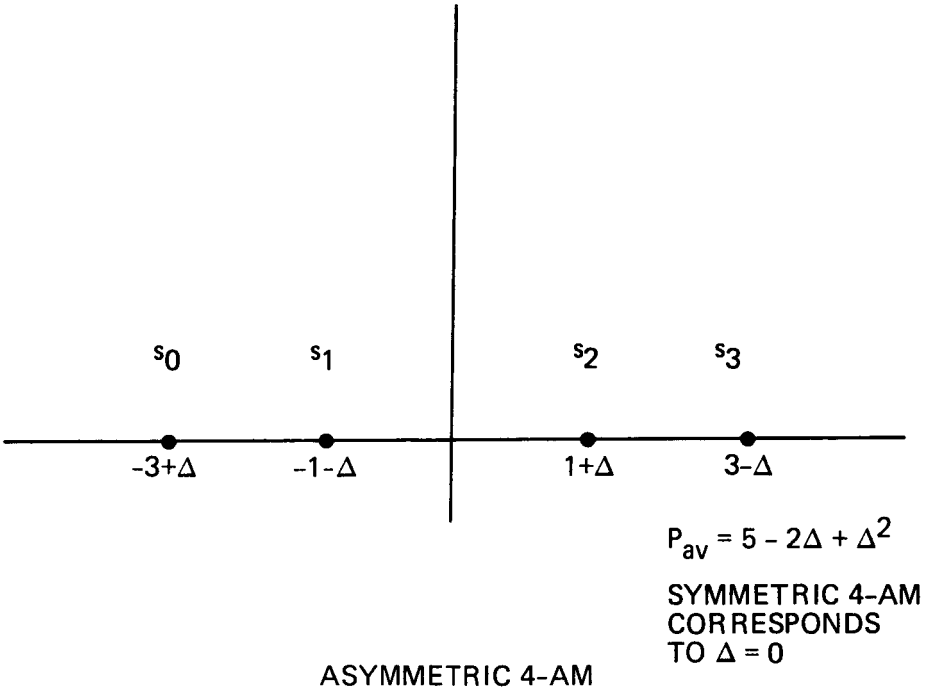

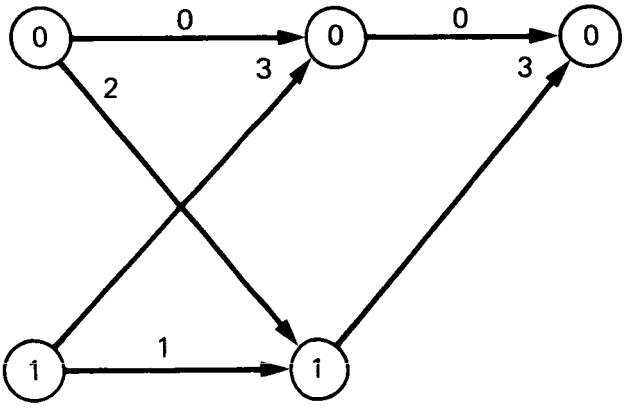

Figure 2. Trellis Diagram for Conventional Rate 1/2 Trellis Coded 4-AM.

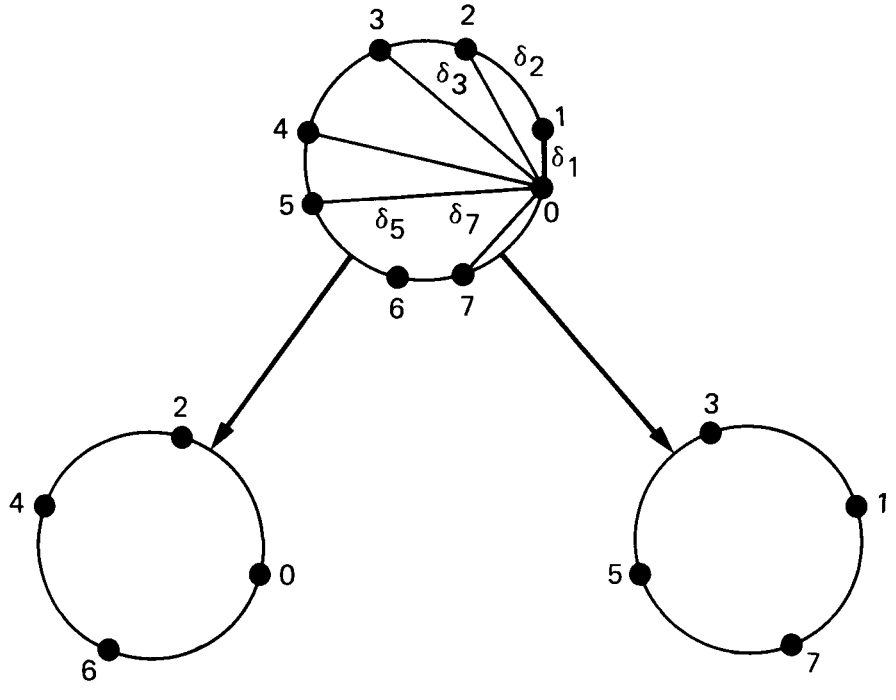

$\delta_1^2 = 4 \sin^2 \frac{\phi}{2} = 2 (1 - \cos \phi)$;

$\delta_2^2 = 2$;

$\delta_3^2 = 4 \sin^2 \left(\frac{\pi}{4} + \frac{\phi}{2} \right) = 2 (1 + \sin \phi)$;

$\delta_4^2 = 4$

$\delta_5^2 = 4 \sin^2 \left(\frac{\pi}{2} - \frac{\phi}{2} \right) = 2 (1 + \cos \phi)$

$\delta_6^2 = 2$

$\delta_7^2 = 4 \sin^2 \left(\frac{\pi}{4} - \frac{\phi}{2} \right) = 2 (1 - \sin \phi)$

Figure 3. Set Partitioning for Asymmetric 8-PSK.

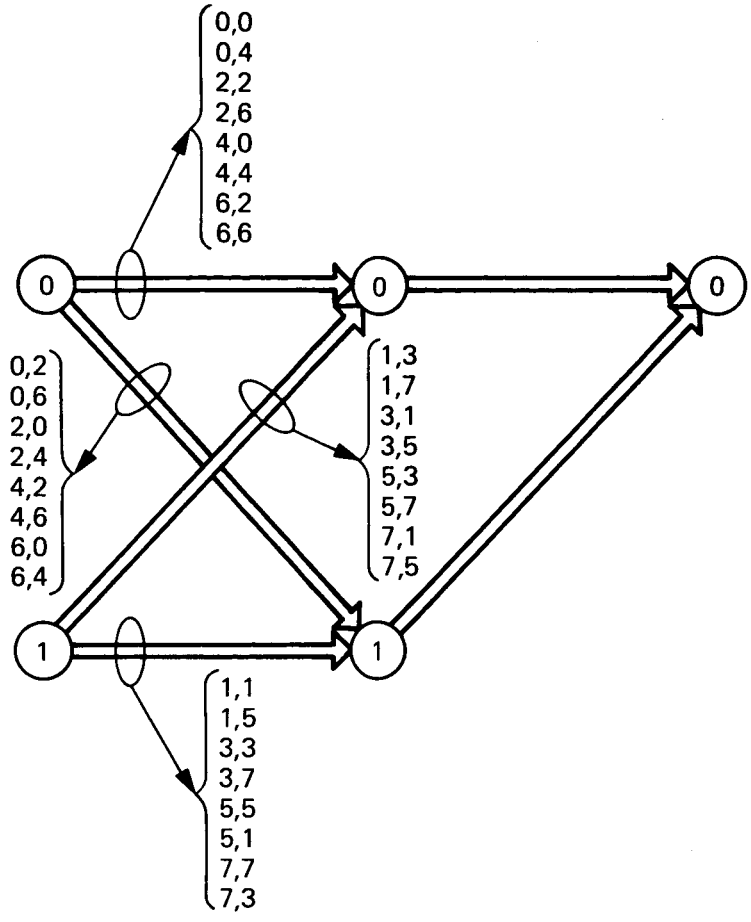

Figure 4a. 2-State Multiple Trellis Diagram for Rate 2/3 Coded 8-PSK and 8-AM; k=2.

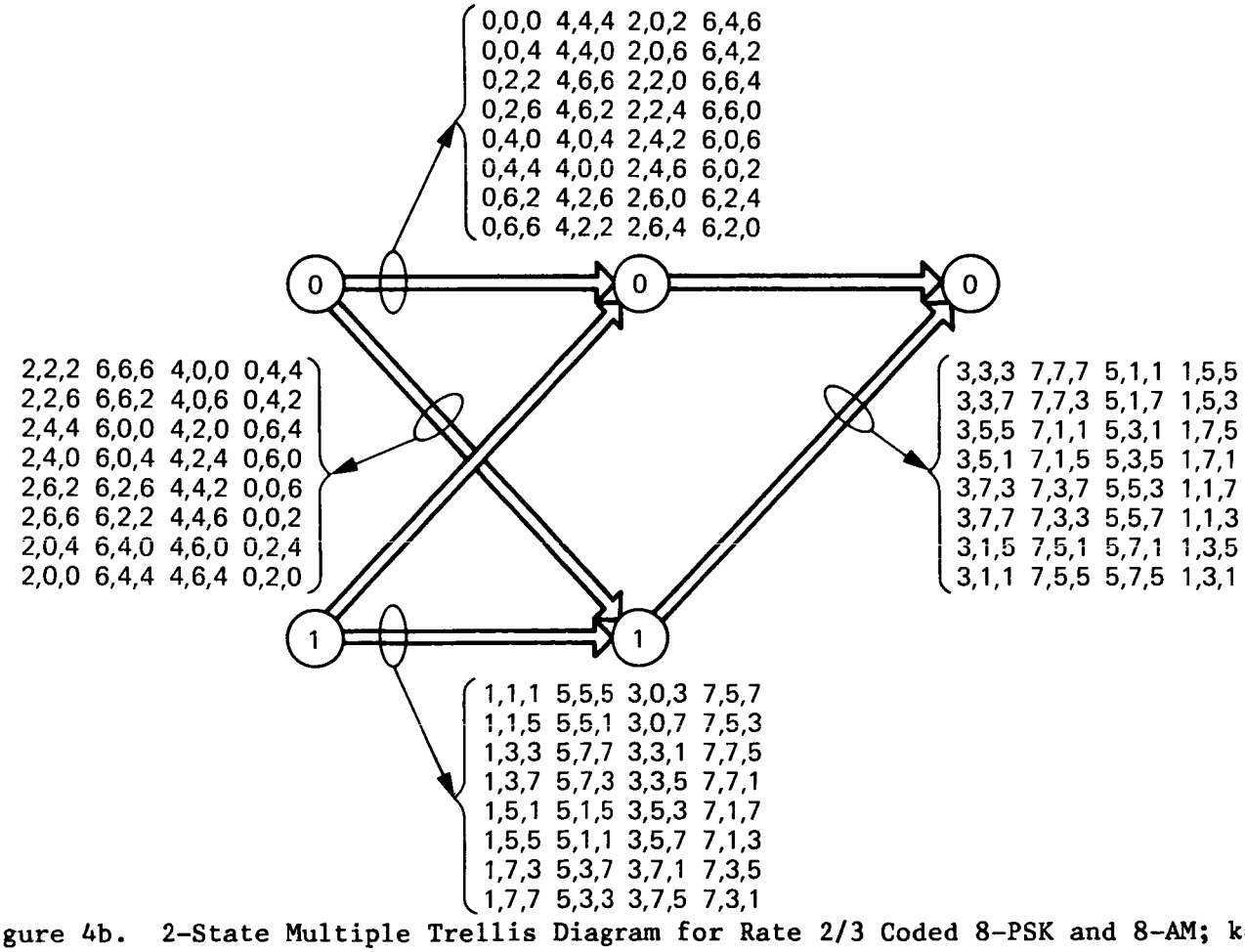

Figure 4b. 2-State Multiple Trellis Diagram for Rate 2/3 Coded 8-PSK and 8-AM; k=3.

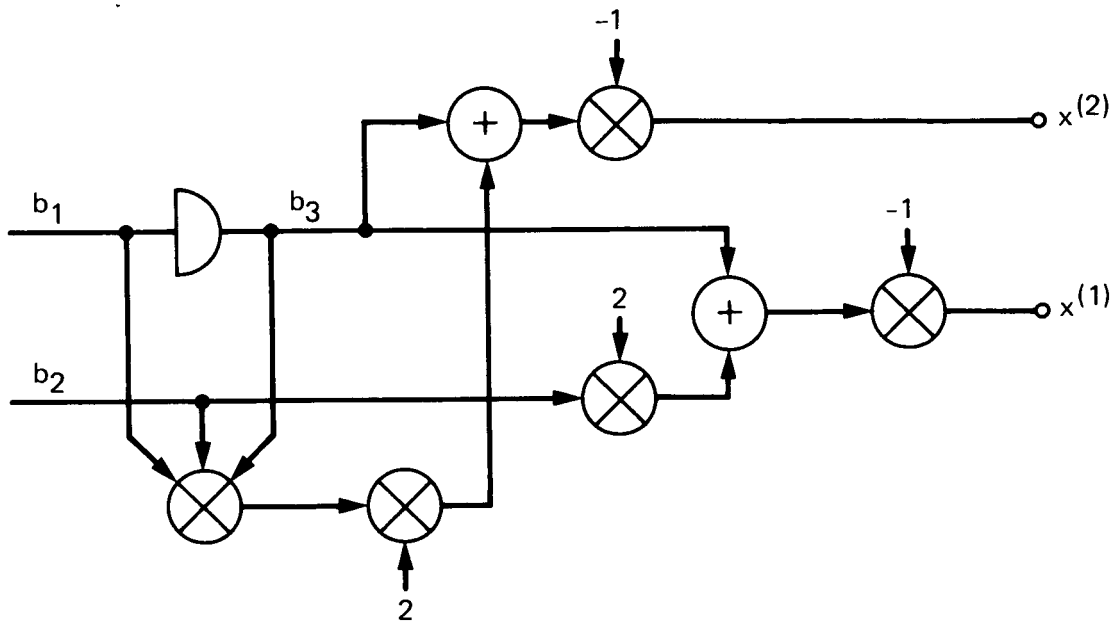

Figure 5. Transmitter Implementation for Rate 1/2 Multiple Trellis Coded 4-AM (2 States); k=2.

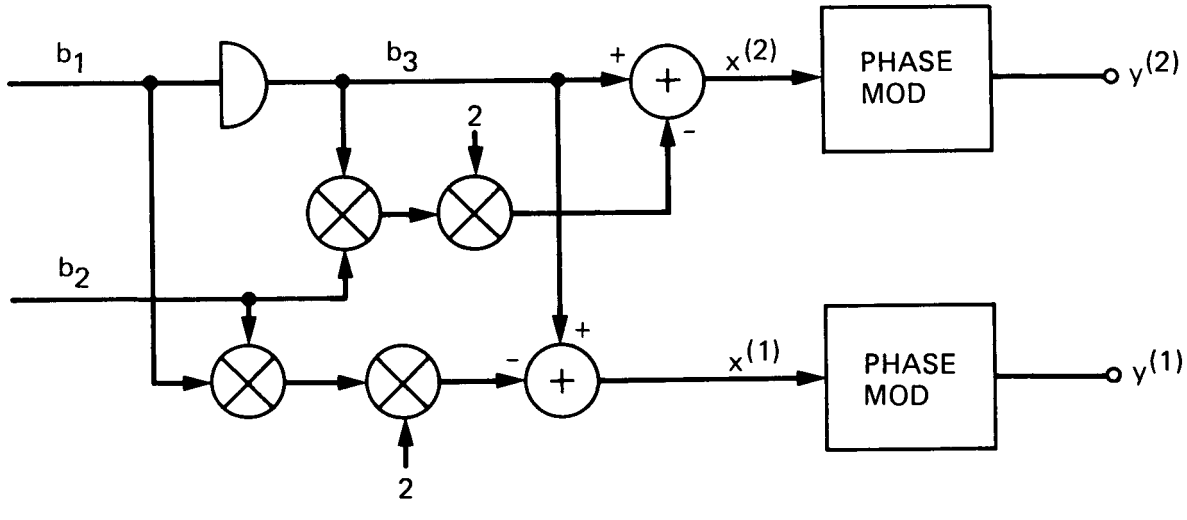

Figure 6. Transmitter Implementation for Rate 1/2 Multiple Trellis Coded QPSK (2 States); k=2.

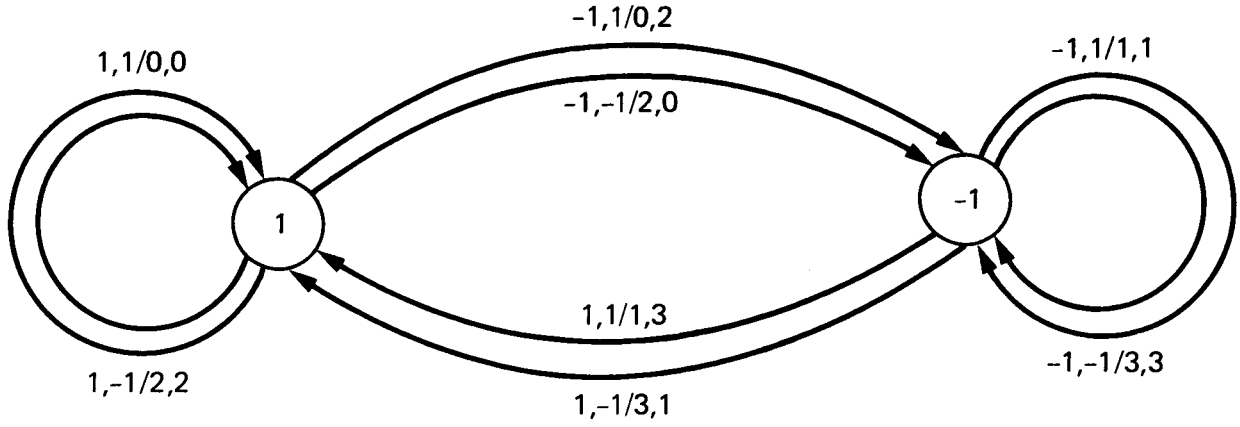

Figure 7. State Diagram for Rate 1/2 Multiple (k=2) Trellis Coded QPSK.

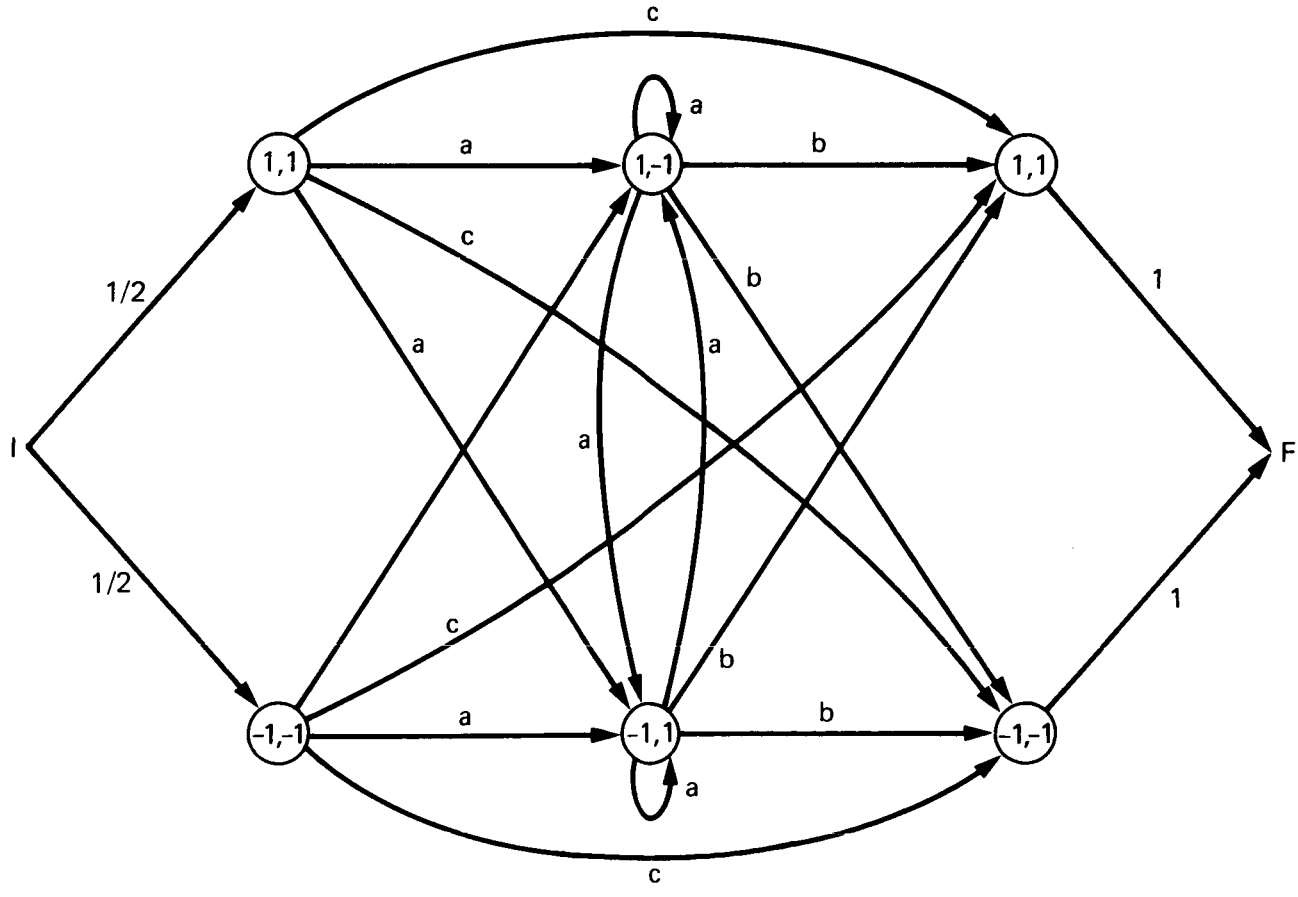

Figure 8. Pair-State Diagram Corresponding to Figure 7.

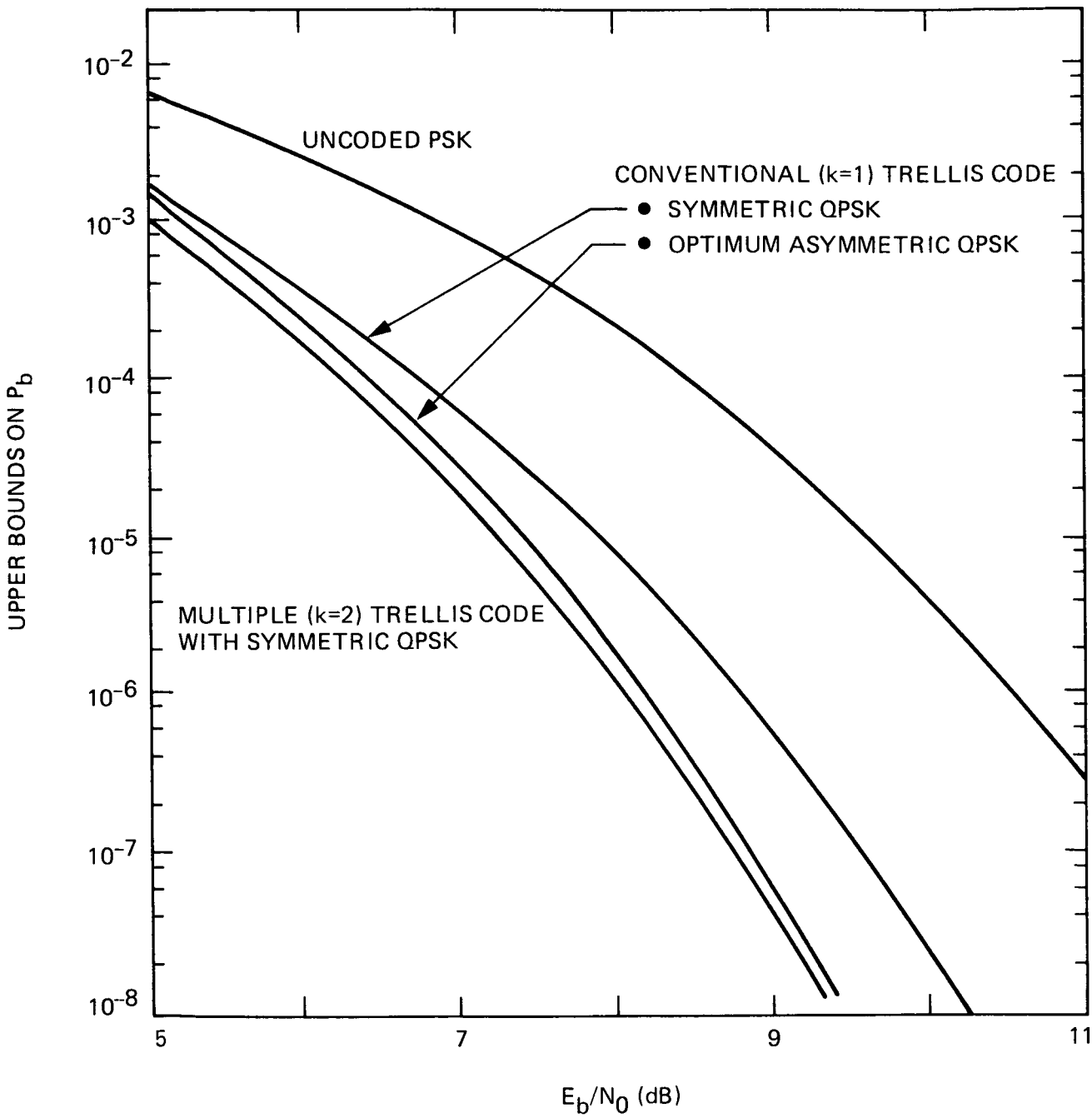

Figure 9. A Comparison of the Performance of Several Rate 1/2 Trellis Coded QPSK Modulations.

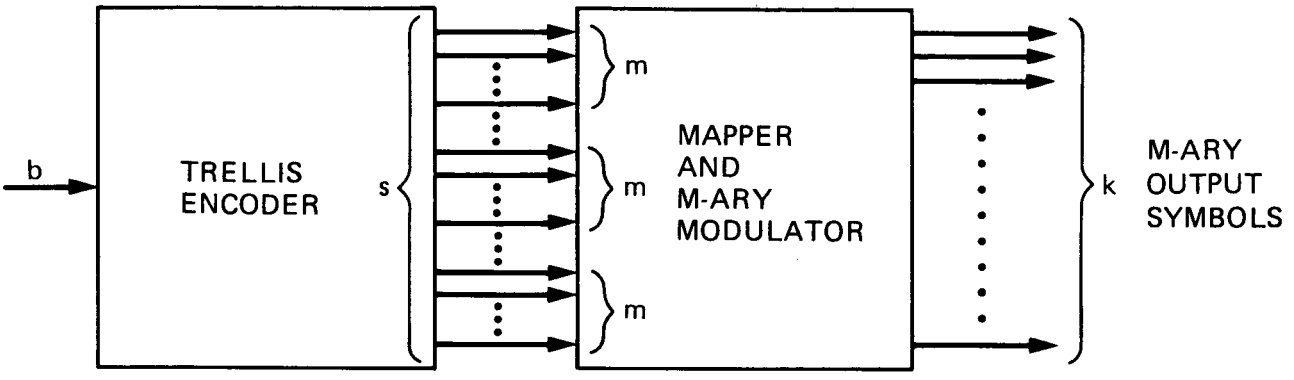

Figure 10. Generalized MTCM Transmitter.

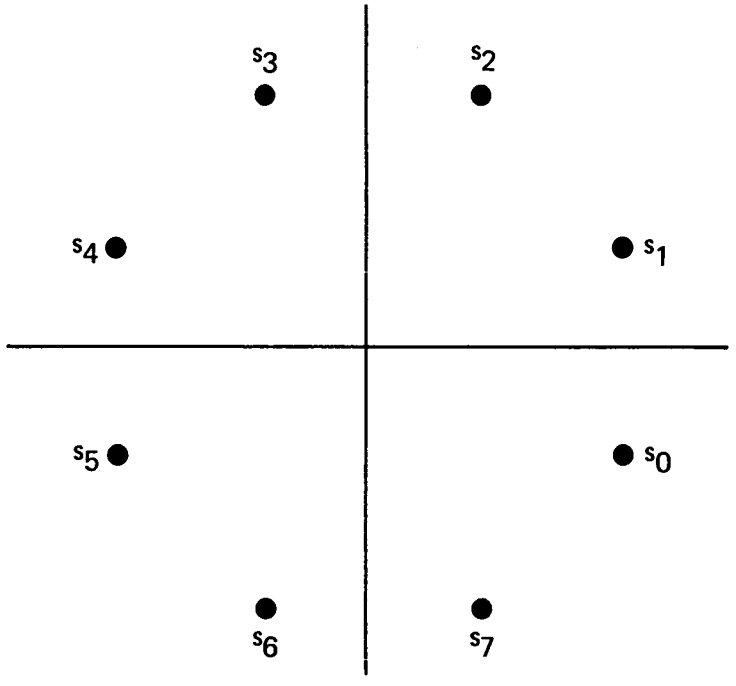

Figure 11. Symmetric 8PSK Signal Set.

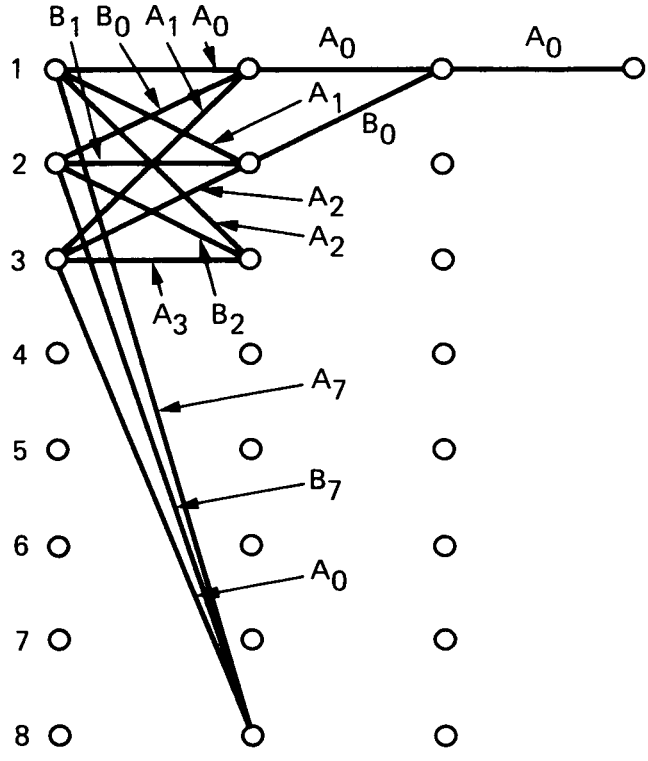

Figure 12. 8-State Trellis Diagram for Example 1.

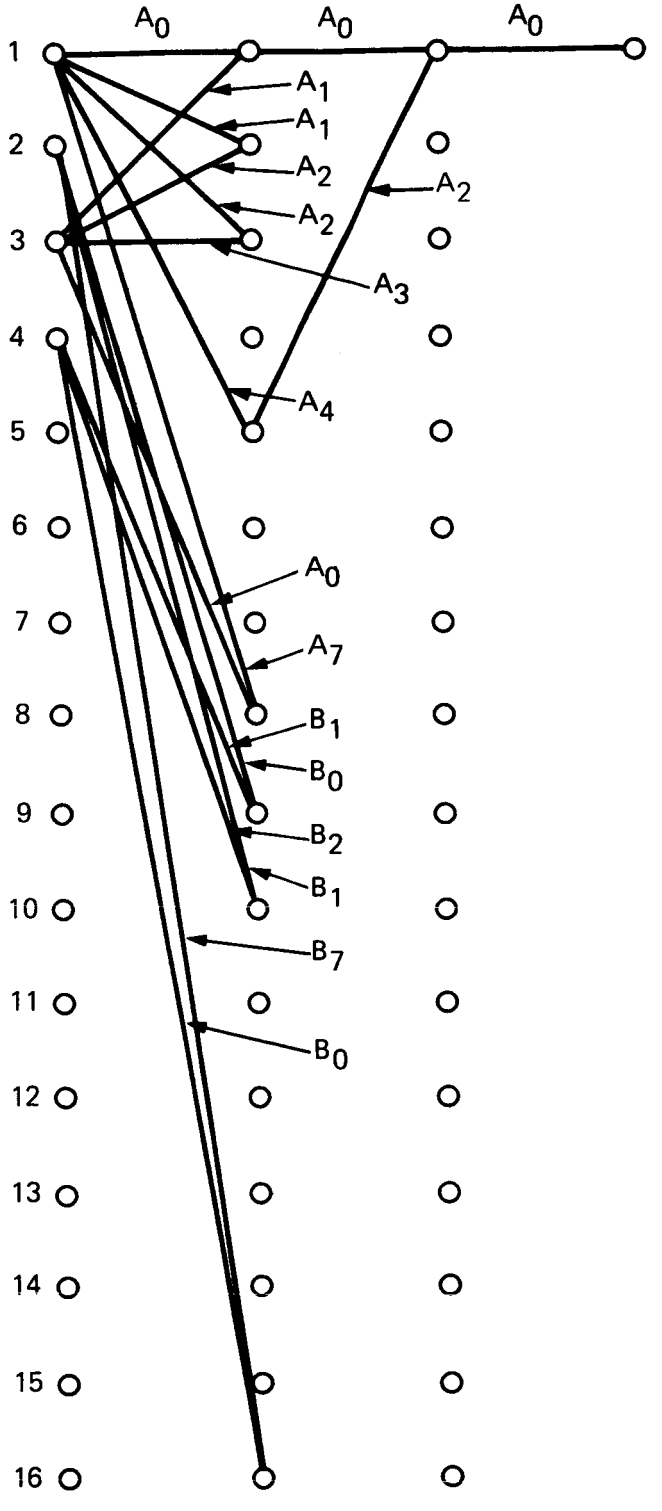

Figure 13. 16-State Trellis for Example 1.

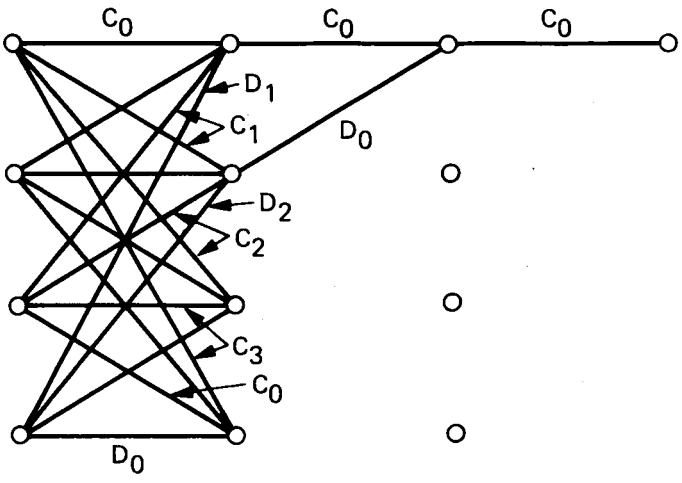

Figure 14. 4-State Trellis for Example 2.

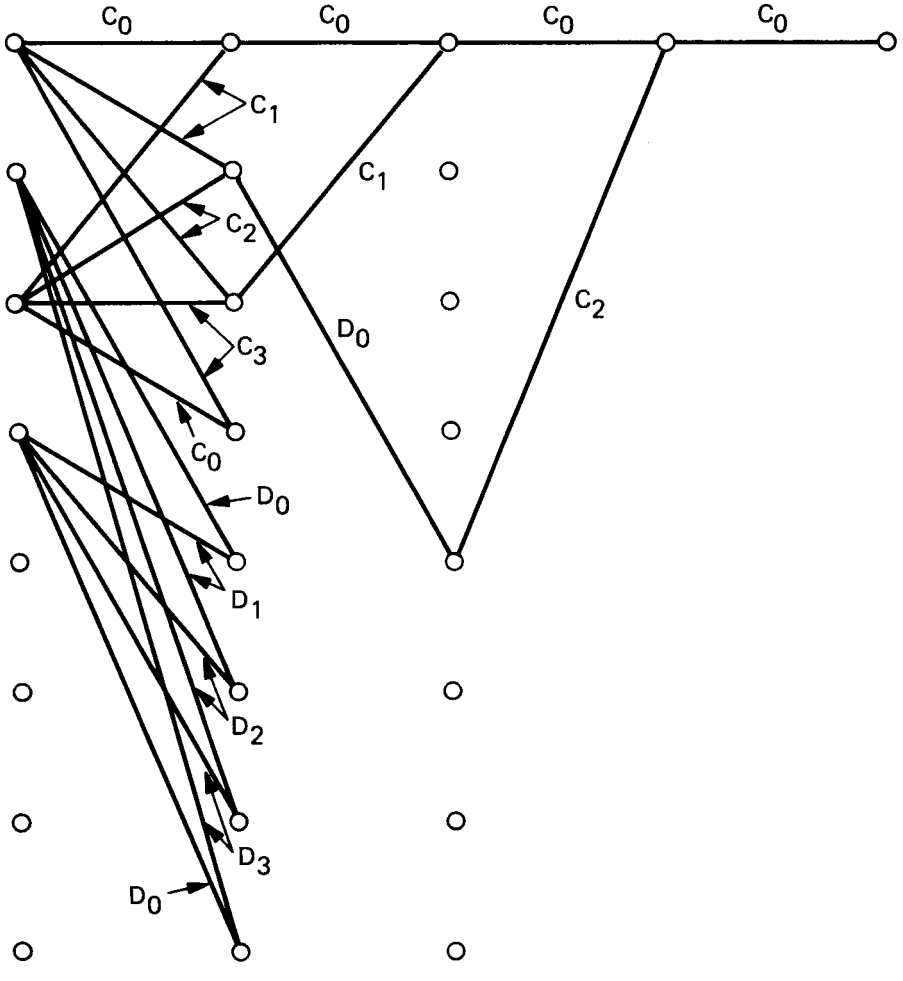

Figure 15. 8-State Trellis for Example 2.

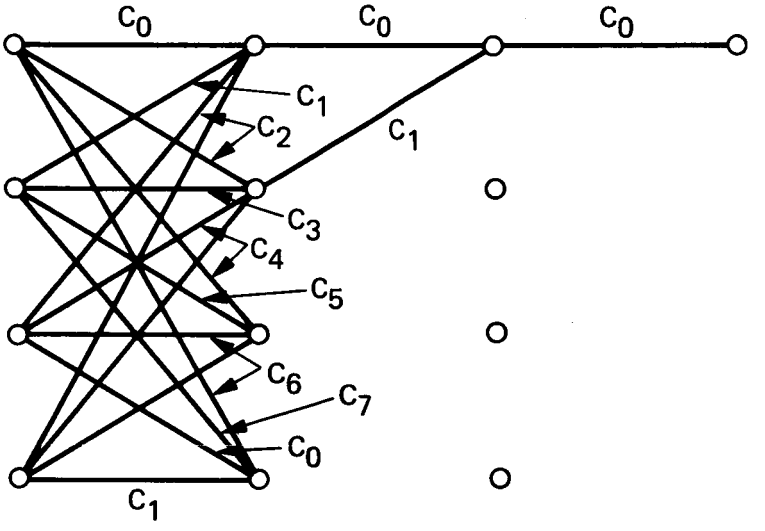

Figure 16. 4-State Trellis for Example 4.

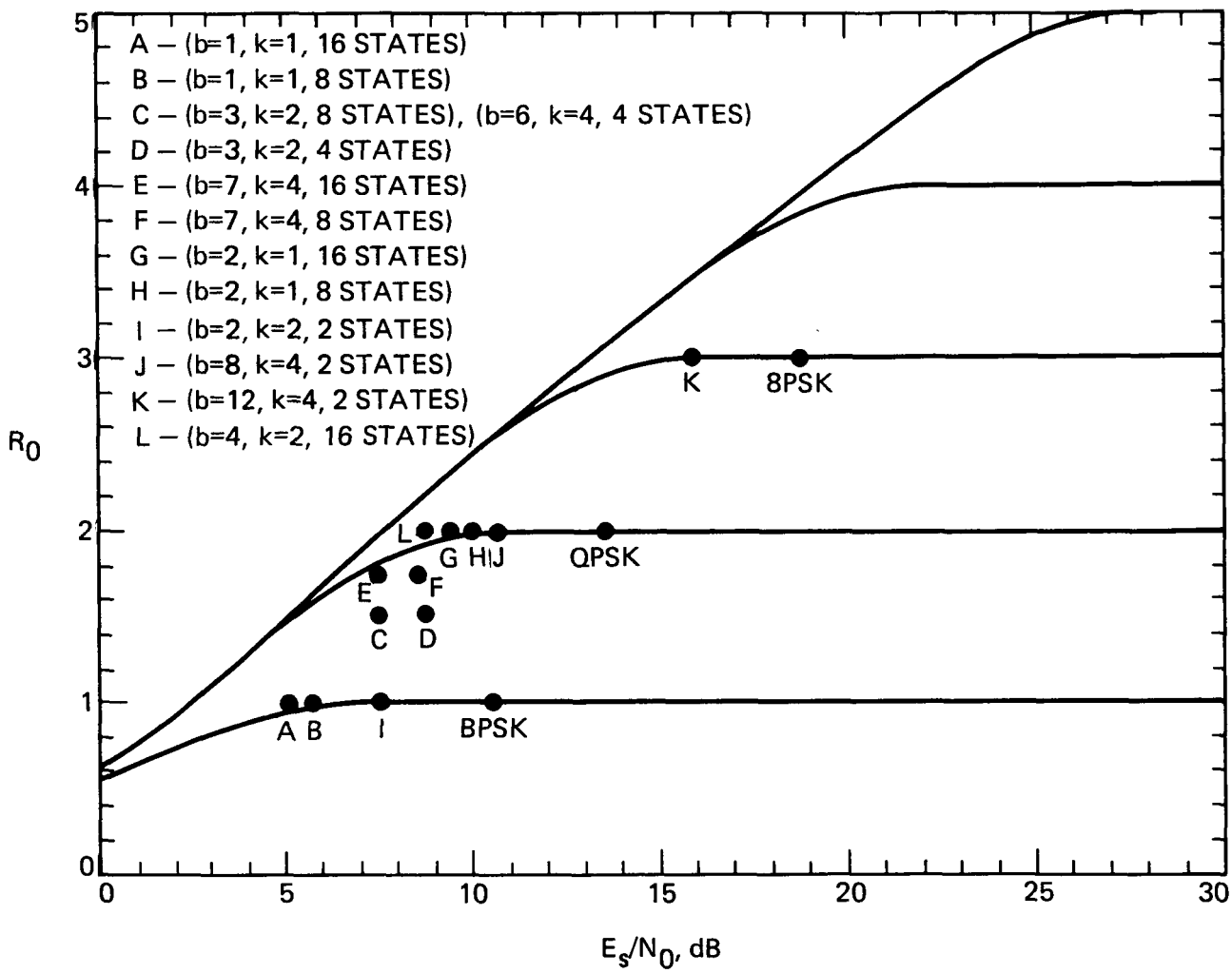

Figure 17. Comparison of Computational Cutoff Rate of MPSK with Throughput Performance of Trellis Coded MPSK